Statistical analysis of nonlinearly propagating acoustic noise in a tube

Michael B. Muhlestein and Kent L. Gee
Brigham Young University, Provo, Utah 84602

Acoustic fields radiated from intense, turbulent sound sources such as military jets and rockets are not well understood. In addition to the inherent random nature of the field, the amplitudes of the acoustic vibration are great enough that nonlinear considerations are necessary for modeling. In order to better understand these complex fields, high-amplitude noise in a tube is measured and analyzed. The basics of nonlinear acoustics will be covered briefly in this talk. Additionally, some statistical tools that are useful in analyzing random systems, such as probability density functions and skewness, will be explained. The measured evolution of the skewness of the first time derivative of high-amplitude noise in a tube will be presented.

I. Motivation

While much is understood concerning the phenomena that affect high-amplitude sound waves, little has been done to understand the nonlinear evolution of high-amplitude random noise.[1,2] Because the radiant sound from the high-speed jets out of rockets[3,4] and military aircraft generate high-amplitude random noise,[5] this is an important problem. The purpose of this paper is to increase understanding of how high-amplitude noise evolves in a plane-wave environment, particularly near its source.

II. Nonlinear and Statistical Theory

A. Nonlinear Theory

High-amplitude propagating acoustic waves are most simply modeled with the inviscid Burgers equation,[6] which gives the implicit solution

$$p = \phi(\tau - \eta x p), \qquad (1)$$

where p is the acoustic pressure, $\phi(t)$ is the source pressure waveform, τ is the retarded time $t - x/c_0$, c_0 is the small signal speed of sound, x is the distance from the source and η is a constant based on the physical properties of the medium, about 40.5×10^6 for air.

This solution gives some quick insight as to the behavior of the sound. As the sound propagates, the compressions (high pressure portions of the waveform) will travel faster than the rarefactions. The physical process that dictates this behavior is the temperature dependence of sound speed. As pressure increases significantly, the temperature also increases, causing an increase of sound speed.

Equation (1) predicts that after a certain distance, called the shock formation distance, the pressure will be multi-valued – there will be multiple pressures at a given location. This is nonphysical, and must be accounted for using another constraint, called weak-shock theory. This uses what is called the equal-area rule. When looking at a graph of the pressure, one can draw a vertical line through the multi-valued region of the waveform. The line that splits the region into two equal-area regions will be the line that represents the true pressure through the region. This discontinuity is called a shock. An example, that of an initially sinusoidal signal, is shown in Fig. 1. On top is the pressure amplitudes, and bottom is its normalized first time derivative.

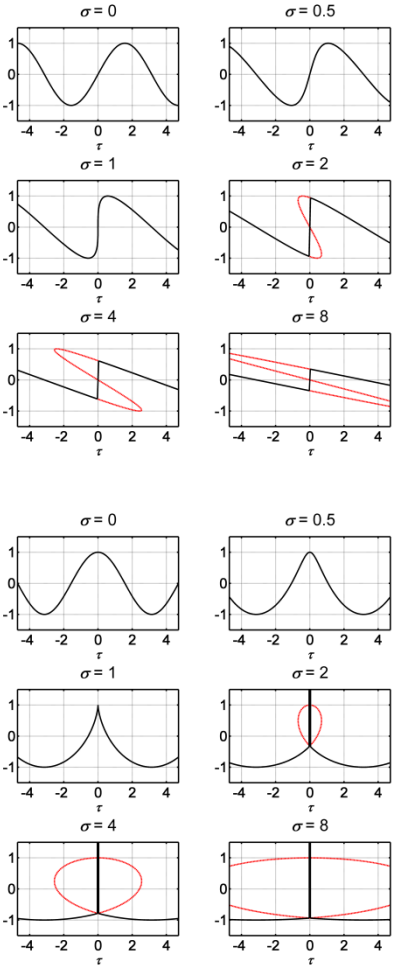

Figure 1. An initially sinusoidal signal's nonlinear evolution. The amplitude is given on the top and the first time derivative is given on the bottom. The various plots are at various values of $\sigma = x/\bar{x}_S$

B. Statistical Theory

Because noise is statistically random, it makes sense to analyze the nonlinear propagation of said noise with statistical tools. Some of these tools will be briefly explained in this section.[7]

Suppose one had a random waveform and chose a single time randomly. The probability that the pressure associated with that time is a pressure between P_1 and P_2 is given

by the integral $\int_{P1}^{P2} \rho(p)dp$, where $\rho(p)$ is the probability density function (PDF). For a sinusoidal signal the PDF is given by

$$\rho_S(p) = \frac{1}{\pi\sqrt{1-a^2}}, \qquad (2)$$

and the PDF for zero mean Gaussian noise is

$$\rho_G(p) = \frac{1}{\sigma_p\sqrt{2\pi}} e^{-x^2/2\sigma_p^2}, \qquad (3)$$

where σ_p is the standard deviation.

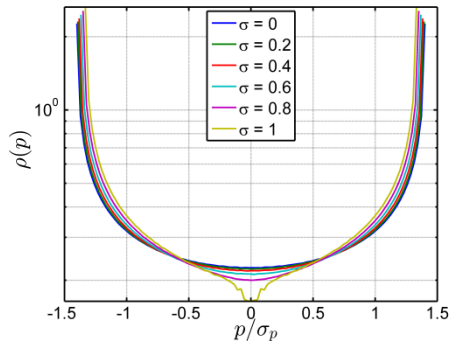

Figure 2. Probability density function of a nonlinearly evolving initially sinusoidal signal at various values of $\sigma = x/\bar{x}_S$. Notice that there is not much change over σ.

As a waveform distorts, the PDF has the possibility of also deforming. However, in the case of the nonlinearly evolving initially sinusoidal signal, the PDF does not change until shocks have begun to form. However, the PDF of the first time derivative of the pressure amplitude of the signal (hereafter just called the pressure derivative; see Fig. 2 for the pressure derivative for an initially sinusoidal signal) does change significantly even at distances well short of the shock formation distance. Estimates of the PDF for a propagating initially sinusoidal signal are examined below in Section III.

There are several ways of analyzing the PDF of a signal called moments. The n[th] moment of a PDF with random variable x is given by

$$\mu_n = \int_{-\infty}^{\infty} x^n \rho(x)dx. \qquad (4)$$

Note that $\mu_0 = 1$ by definition. The first moment is the mean and is assumed to be zero for acoustic signals. The square root of the second moment is the standard deviation, often written σ_p, and is equal to the rms amplitude of the signal. The skewness of a signal is $S_p = \mu_3/\sigma_p^3$, and gives an indication of the asymmetry of the signal.

Since the probability density function does not change significantly before the shock formation distance, the standard deviation and the skewness are also left essentially unchanged for a propagating initially sinusoidal signal. However, both of these moments change dramatically for the pressure derivative.[8] Since the present paper emphasizes S_{p_t}, the skewness of the pressure derivative, a plot of S_{p_t} as a function of normalized distance is shown in Fig. 3.

It should be noted that because the above analysis is only valid for completely lossless media, it does not apply to the measurements discussed below. However, the general trends should be the same. The most notable effect of physical systems would be the delay of shock formation.[9] It will be apparent that the rapid increase of the S_{p_t} will occur at a distance of $x/\bar{x}_S > 1$.

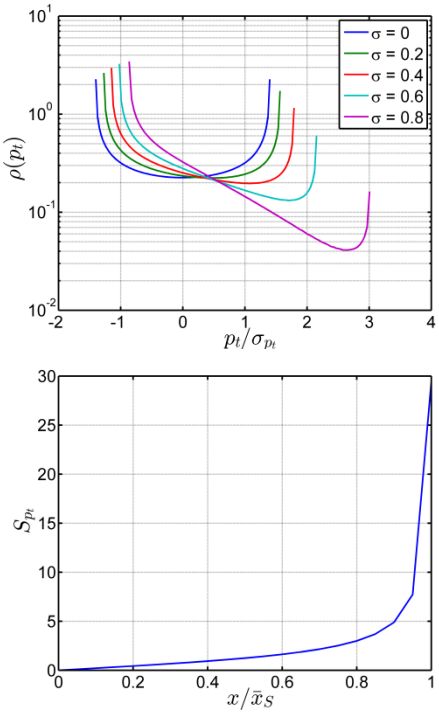

Figure 3. Probability density function of the first time derivative of a nonlinearly evolving initially sinusoidal signal at various values of $\sigma = x/\bar{x}_S$ (top) Also, the skewness of the same (bottom).

III. Nonlinear Noise Propagation

The distance at which a shock is first formed anywhere in the time waveform is defined as the shock formation distance, as stated above. For a random noise signal this distance is ill defined and varies from signal to signal as pressure outliers change. However, there are distances at which the statistical characteristics of the waveform greatly resemble that of an initially sinusoidal signal. We will call this the characteristic shock formation distance. We would expect that as the bandwidth of the random noise went to zero we would retrieve the shock formation distance for an initially sinusoidal signal with peak amplitude p_0 and angular frequency ω:

$$\bar{x}_S = \frac{\eta}{p_0\omega}. \qquad (5)$$

Note that $\bar{x}$ will be used to denote a generic shock formation distance in this paper.

A nonlinear distortion length was defined by Gurbatov and Rudenko[10] for analysis of the nonlinear evolution of random narrowband noise

$$\bar{x}_N = \frac{\eta}{\sigma_p\omega_0}, \qquad (6)$$

where ω_0 is the characteristic or central frequency of the noise. It should be noted that the central frequency was determined as the arithmetic mean of the upper and lower spectral limits.

The nonlinear distortion length in Eq. 6 is an attractive candidate for the characteristic shock formation distance since it is so similar in form to Eq. 5. However, since the amplitude term is the rms amplitude, it will be at best off by a factor of square root of two. To account for that and any other multiplicative discrepancies found by using noise rather than a sinusoidal signal, we will write

$$\bar{x}_\kappa = \frac{\bar{x}_N}{\kappa} = \frac{\eta}{\kappa\sigma_p\omega_0}, \qquad (7)$$

where κ is yet to be determined. One physical interpretation of κ is the number standard deviations of the pressure amplitudes which gives the equivalent peak amplitude of the noise signal.

To check the utility of $\bar{x}_\kappa$ as a characteristic shock formation distance, a plane wave tube was built to experimentally examine shock formation in random noise signals. The tube was constructed out of 2.54 cm radius (2 in. diameter) PVC pipe, about 20 m in 3.048 m segments connected with rigid PVC couplers. The tube was driven with a BMS 4591 compression driver. To sample the propagating acoustic waves, holes were drilled in the pipe at distances 0.35, 2.55, 5.59, 8.63 and 11.7 m from the source, inside which were placed 3.175 mm (1/8 in.) G.R.A.S. microphones. By varying the amplitude of the signal a continuum of values of $x\backslash\bar{x}$ is possible to be measured.

Several types of signal were analyzed. As a benchmark, an initially sinusoidal signal was used. Both broadband and narrowband Gaussian noise signals were also used. Finally, since the noise that radiates from rocket jets is slightly skewed positively from a Gaussian signal, noise with jet-like statistics were also used. The jet-like noise had the same initial spectra as the broadband noise.

In Figs. 4-6 typical measurement results are showed. Figure 4 gives the pressure waveform for an initially sinusoidal signal (top) and a narrowband noise signal (bottom) at both the first and last microphone locations. Nonlinear waveform deformation is readily apparent in both cases. Figure 5 gives typical spectra for the initially sinusoidal, narrowband and broadband signals at the first microphone (top) and last microphone (bottom) locations. Because the nonlinear waveform deforms it to have steeper slopes, higher frequency content is being generated at longer distances.

In Fig. 6 is shown the estimates of the PDF at each microphone location for initially sinusoidal (top) and narrowband Gaussian noise (bottom) signals. In all cases narrowband noise looks statistically very similar to broadband noise. Notice that the general shape of the PDF estimate does not change much over distance for either case. There is a little bit of a shift of the negative edge toward the positive side. This is a result of boundary effects of the tube,[9] which was not accounted for in the analysis in Section II. Because it does not vary substantially with distance, this will not be a good way to find the characteristic shock formation distance.

In Fig. 7 is shown the PDF estimates of the pressure derivatives for initially sinusoidal (top) and narrowband Gaussian noise (bottom) signals. The extremity of the positive outliers becomes grows larger for larger distances from the source. This can be better seen in the plot of S_{p_t} as a function of $x/\bar{x}_S$ and $x/\bar{x}_N$ for initially sinusoidal and Gaussian noise, respectively, shown in Fig. 8.

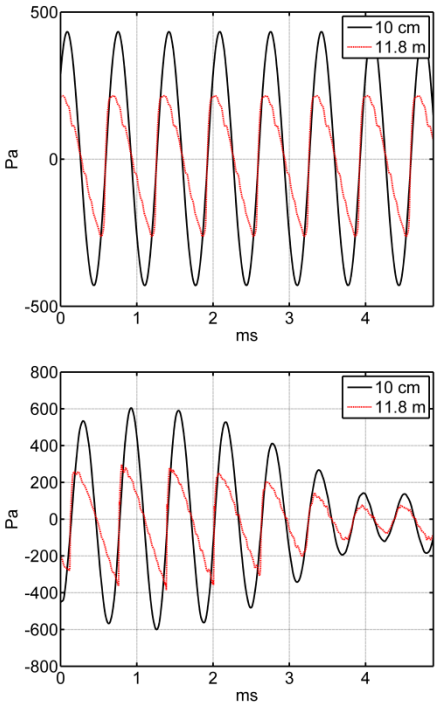

Figure 4. Typical measured waveforms at the first and last microphones. Top, an initially sinusoidal signal; bottom, an initially Gaussian narrowband signal. Nonlinear waveform deformation is clearly visible in both.

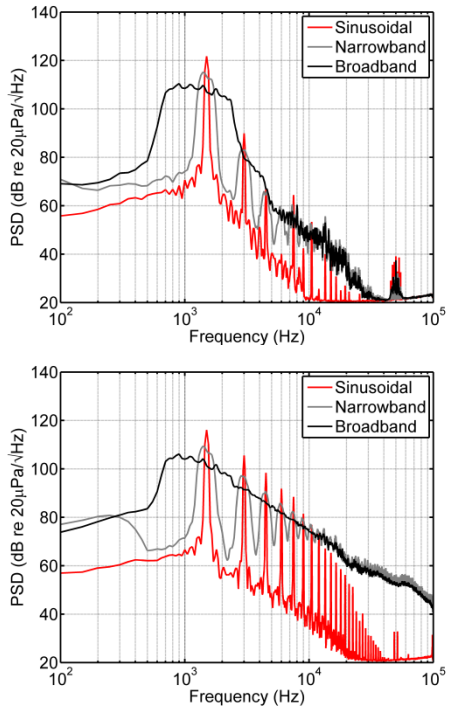

Figure 5. Typical measured spectra at the first (top) and last microphones (bottom) for initially sinusoidal, narrowband and broadband signals. Nonlinear high-frequency generation is evident.

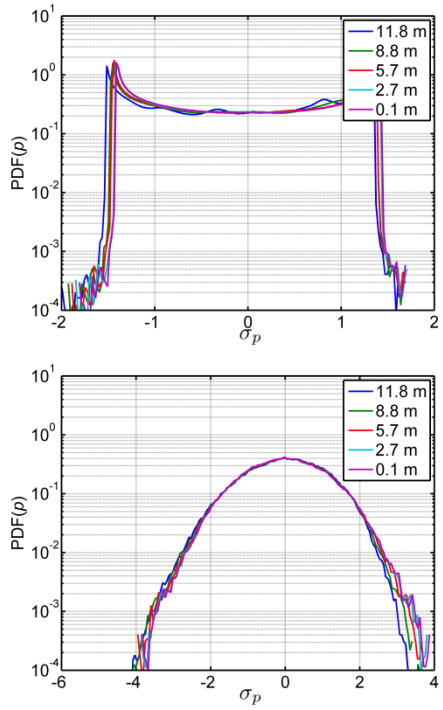

Figure 6. Typical PDF estimates for evolving signals. On the top, initially sinusoidal and, on the bottom, initially Gaussian narrowband.

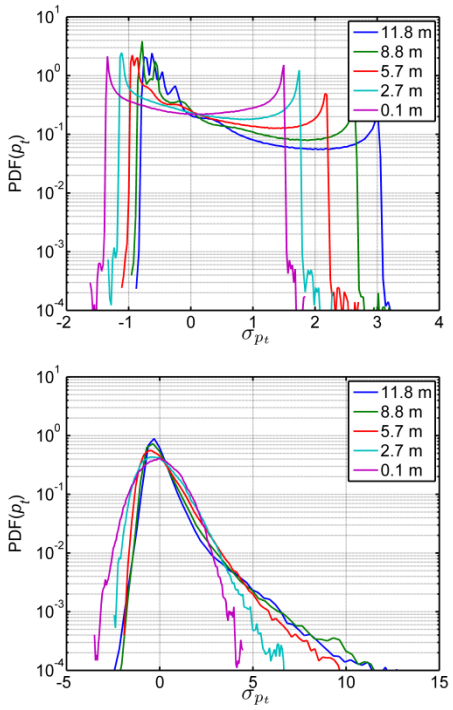

Figure 7. Typical PDF estimates for evolving signals' first time derivatives. On the top, initially sinusoidal and, on the bottom, initially Gaussian narrowband.

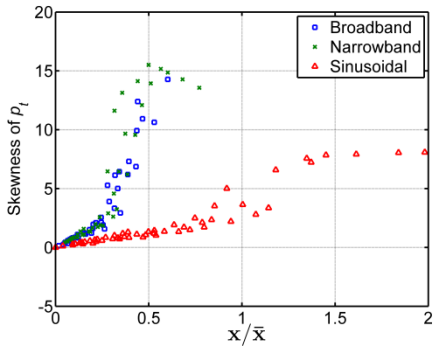

Figure 8. Skewness of the pressure derivative for various types of initial signals as a function of $x/\bar{x}$. For initially sinusoidal, $\bar{x} = \bar{x}_S$, and for initially Gaussian, $\bar{x} = \bar{x}_N$.

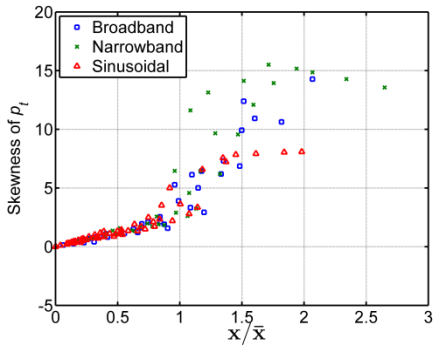

Figure 9. Skewness of the pressure derivative for various types of initial signals as a function of $x/\bar{x}$. For initially sinusoidal, $\bar{x} = \bar{x}_S$, and for initially Gaussian, $\bar{x} = \bar{x}_\kappa$.

It is easily seen that the form of S_{p_t} is generally the same for both initially sinusoidal and Gaussian noise signals of both narrowband and broadband types, and both similar to the lossless prediction found in Fig. 3. Using the skewness of the pressure derivative as a figure of merit, we would expect the two curves of S_{p_t} to follow each other much more closely if we were using the characteristic shock formation distance instead of $\bar{x}_N$. Notice that there seems to be a multiplicative factor off between the two curves. If this is the only significant discrepancy, then we can use $\bar{x}_\kappa$ (Eq. 7) as an estimate of the characteristic shock formation distance, where κ will be determined using a least-squares fit. A plot of the skewness of the pressure derivative as a function of $x/\bar{x}_S$ for the initially sinusoidal case and as a function of $x/\bar{x}_\kappa$ is shown in Fig. 9

The three curves shown in Fig. 9 fall on top of each other nicely in the region before the rapid increase near the assumed shock formation distance. In order to get the best fit, separate least-squares fits were used for each type of noise and each microphone location, thus yielding different values for κ. All values of κ from this point in the paper on will be found with the microphone closest to the source, to remove as many boundary-layer effects of the tube as possible. In order to see what sort of frequency dependence the parameter κ has, the same test was performed for several central or characteristic frequencies. A plot of $\kappa(f)$ for narrowband, broadband and jet-like noise is given in Fig. 10.

From Fig. 10 it appears that there is some spectral dependence of κ. As the frequency increases, the value of κ decreases. While the first cutoff frequency of the tube precludes experiments to much higher frequencies, it is to be expected that κ will never drop below $\sqrt{2}$ for any frequency. There does not seem to be much dependence on bandwidth. This comes from the fact that the narrowband and broadband Gaussian noise lines are very close to each other and follow the same trends. Notice, however, that κ for the jet-like noise is consistently higher than for the other two types of noise. Thus, it is to be expected that there is also significant dependence of the parameter κ with respect to initial pressure statistics. This statistical dependence has not been well studied yet.

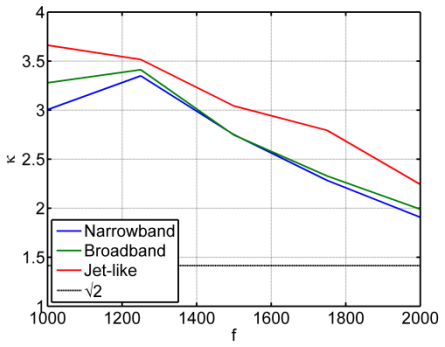

Figure 10. Variation of the parameter κ as a function of frequency. The value of $\sqrt{2}$ is also plotted for reference.

IV. Conclusions

Due to its random nature, there is little utility in the use of the shock formation distance to describe the nonlinear evolution of noise radiated from high-speed jets like those generated by rockets. A characteristic shock formation distance can be of more utility. As an example of its utility, the characteristic shock formation distance does not change for two random but statistically identical noise waveforms. This may allow one to define acoustic distances which can be used for physically meaningful non-dimensionalization. This characteristic shock formation distance appears to be frequency and initial statistics dependent.

V. Bibliography

[1]D. F. Pernet and R. C. Payne, "Non-linear propagation of signals in air," J. Sound Vib. 17 (3), 383-396 (1971).

[2]O.V. Rudenko, “Interactions of intense noise waves,” Sov. Phys. Usp. **29**(7) 620 – 641(1986).

[3]K.L. Gee, J.H. Giraud, J.D. Blotter, and S.D. Sommerfeldt, “Energy-based acoustical measurements of rocket noise,” in *15th AIAA/CEAS Aeroacoustics Conference* (AIAA, Miami, Florida, 2009).

[4]S. A. McInerny and S. M. Olcmen, "High-intensity rocket noise: Nonlinear propagation, atmospheric absorption, and characterization," J. Acoust. Soc. Am. **117** (2), 578-591 (2005).

[5]K. L. Gee, A. A. Atchley, T. B. Gabrielson, and V. W. Sparrow, "Preliminary Analysis of Nonlinearity in Military Jet Aircraft Noise Propagation," AIAA Journal **43** (6), 1398-1401 (2005).

[6]D. T. Blackstock, M. F. Hamilton, and A. D. Pierce, "Progressive Waves in Lossless and Lossy Fluids", in *Nonlinear Acoustics*, edited by M. F. H. and D. T. Blackstock (Academic Press, 1998), pp. 65-150.

[7]J. S. Bendat and A. G. Piersol, *Random Data*. (2010), Fourth ed.

[8]M. R. Shepherd, K. L. Gee, and A. D. Hanford, "Evolution of statistical properties for a nonlinearly propagating sinusoid," J. Acoust. Soc. Am., in press (2011).

[9]M. F. Hamilton, Yu. A. Il'inskii, and E. A. Zabolotskaya, "Dispersion", in *Nonlinear Acoustics*, edited by M. F. Hamilton and D. T. Blackstock (1998), pp. 151-175.

[10]S. N. Gurbatov and O. V. Rudenko, "Statistical Phenomena", in *Nonlinear Acoustics*, edited by M. F. Hamilton and D. T. Blackstock (Academic Press, 1998), pp. 377-398.